Biosensors and Bioelectronics 105 (2018) 58–64

Contents lists available at ScienceDirect

Biosensors and Bioelectronics

journal homepage: www.elsevier.com/locate/bios

The field effect transistor DNA biosensor based on ITO nanowires in label-free hepatitis B virus detecting compatible with CMOS technology

Mohsen Shariati

Institute for Nanoscience and Nanotechnology, Sharif University of Technology, Tehran 14588-89694, Iran

ARTICLE INFO

Keywords:
DNA biosensor
Hepatitis B virus
Field effect transistor
Indium tin oxide nanowires
Label free detection

ABSTRACT

In this paper the field-effect transistor DNA biosensor for detecting hepatitis B virus (HBV) based on indium tin oxide nanowires (ITO NWs) in label free approach has been fabricated. Because of ITO nanowires intensive conductance and functional modified surface, the probe immobilization and target hybridization were increased strongly. The high resolution transmission electron microscopy (HRTEM) measurement showed that ITO nanowires were crystalline and less than 50 nm in diameter. The single-stranded hepatitis B virus DNA (SS-DNA) was immobilized as probe on the Au-modified nanowires. The DNA targets were measured in a linear concentration range from 1fM to 10 μM. The detection limit of the DNA biosensor was about 1fM. The time of the hybridization process for defined single strand was 90 min. The switching ratio of the biosensor between "on" and "off" state was ~ 1.1×10^5. For sensing the specificity of the biosensor, non-complementary, mismatch and complementary DNA oligonucleotide sequences were clearly discriminated. The HBV biosensor confirmed the highly satisfied specificity for differentiating complementary sequences from non-complementary and the mismatch oligonucleotides. The response time of the DNA sensor was 37 s with a high reproducibility. The stability and repeatability of the DNA biosensor showed that the peak current of the biosensor retained 98% and 96% of its initial response for measurements after three and five weeks, respectively.

1. Introduction

The development of DNA detection technology has been the subject of intensive attentions for wide applications, including detecting DNA-based gene sequences (Labuda et al., 2010), identifying clinical diagnosis, nano-bioengineering and food science areas, (Taylor et al., 2006). For DNA detection and sensing, several techniques, such as electrochemical (Zhang et al., 2010), optical fiber sensors (Parab et al., 2010), SPR (surface plasmon resonance) biosensors methods, have been extensively researched. Especially, for achieving success in healthcare science, scientists will mainly depend on the successful knowledge of the pathological diagnosis.

Viral hepatitis caused by hepatitis B virus is regarded as a serious public health problem of worldwide importance, and causes other harmful consequences including cirrhosis and hepatocellular carcinoma, (Wright and Lau, 1993; Mahoney, 1999; Erdem et al., 1999; Nikoobakht and El-Sayed, 2003; Sipova et al., 2010; Han et al., 2013). Over 400 million people in the world have been infected by the HBV and this virus effects on the mortality caused by liver disease which has infected around 1 million annually (Mahoney, 1999). Recently, the intensive attentions have been centralized on the HBV detection and quantification systems development (Shakoori et al., 2015). The nanotechnology and nanoscience-based methods have achieved successes significantly in HBV detection biosensor systems, (Shakoori et al., 2015).

The main challenge to improve the DNA bio-sensing in detection performance is to enhance the DNA probe immobilization capability and its accessibility with DNA target for hybridization process. For solving the probe immobilization problems and their hybridization with target, scientists have used the metal oxide & metal nanoparticles and nanowires, (Wenga et al., 2013). Nanowires with large surface to volume ratio improve the DNA sensor performance (Shakoori et al., 2015; Shariati and Alishavandi, 2014). The enhancement of the DNA immobilization in electrochemical DNA biosensor with colloidal 16 nm gold nanoparticles was reported (Shakoori et al., 2015).

The increase of immobilization of ss-DNA to silica and colloidal Ag surfaces were successfully reported, (Zhang et al., 2004; Fu et al., 2005). However, nanowires have more numerous advantages in comparison to nanoparticles. In order to get higher sensitivity in lower detection limits, NWs can transfer electron more rapidly than NPs and increase the light scattering, (Jia et al., 2007).

Among significant metal oxide nanowires, ITO nanowire has been the subject of wide researches due to its high sensitiveness and detective application, (Shariati and Darjani, 2016; Shariati, 2017). When the

E-mail address: shariatimohsen59@gmail.com.

https://doi.org/10.1016/j.bios.2018.01.022
Received 22 October 2017; Received in revised form 2 January 2018; Accepted 10 January 2018
Available online 11 January 2018
0956-5663/

analytical bio-molecules are adsorbed to distinctive identification bio-molecules on the nanowires surface, the ITO nanowires bio-sensing mechanism materialize changes in current due to a field-effect process, (Cui et al., 2001; Patolsky et al., 2006; Du et al., 2009; Shariati, and Alishavandi, 2014).

By miniaturizing through nanowires, biological sensors have been upgraded, (Wenga et al., 2013). large number of advantages are related to these nano-biosensors such as; reduction of sample and reagent consumption, the sensitivity enhancement, wide availability, fabrication of the cost-effective detectors in mass production, under-controlled ability, portable capability and much faster responsivity (Furuberg et al., 2008).

In this paper, we describe in label-free approach a field-effect transistor DNA biosensor based on ITO nanowires for detecting HBV compatible with CMOS technology. In this work, we will show that the fabricated biosensor is potentially suitable for detecting the HBV DNA sequences. Here, as a proof of concept, the 25-mer non-complementary, mismatched and complementary DNA strands were exposed to fabricated biosensor and the results demonstrated the precise and quick responses of the biosensor. The DNA target was measured in a linear concentration range from 1fM to 10 μM. The detection limit of the DNA biosensor was about 1fM. In addition, the biosensor showed highly satisfied specificity for distinguishing complementary DNA from non-complementary and mismatched DNA sequences.

2. Materials and methods

2.1. DNA materials

The initial stock solutions of the DNA sequences were in concentration around 100 μM and they were prepared with sterile distilled water (SD water) and stored at a fridge at −25 °C. The sequence of DNA sequences was specified by using the BLAST (basic local alignment search tool) to materialize the most satisfied resemblance to the human serum genome. The DNA sequences materialized in our research were followed:

Sequence name	Sequence of oligonucleotides	Company (Country)
Thiolated-probe	5′ - HS (CH2)6 TAC CGT CCC CTT CTT CAT CTG CCG T- 3′	Bioneer Corporation (South Korea)
Target	5′ - ACG GCA GAT GAA GAA GGG GAC GGT A − 3′	Bioneer Corporation (South Korea)
One-point Mismatch	5′ - ACG CCA GAT GAA GAA GGG GAC GGT A − 3′	Bioneer Corporation (South Korea)
Noncomplementary	5′ - TAC CGT CCC CTT CTT CAT CTG CCG T − 3′	Bioneer Corporation (South Korea)

Stock solutions of DNA sequences were prepared in PBS solution (100 mM, pH =7.4) and preserved in a freezer-refrigerator (−25 °C). The preparation of all the stoke solutions were performed by applying the DDW (double de-ionized water).

2.2. Fabrication of ITO nanowires FET device

For fabricating the ITO nanowires FET device, firstly we prepared the FET template. The Si ((100), p-type) was used as substrate. The Si substrate was covered by SiO_2 thin layer in 200 nm thickness. The thickness was controlled by a quartz crystal holder and film thickness monitor in sputtering deposition system. Desk sputtering-thermal deposition system – DST2T model, was set up by the Nano-Structured Coatings Co. (Iran)). On the SiO_2 thin layer surface, gold thin film in 2 μm thickness was deposited as electrodes. Finally the indium and tin thin films were sputtered on the gold film with a sputtering frequency of 13.56 MHz. The purity of all metals was 99.999%. This setup of thin films was performed in three paces, first indium was sputtered, second tin and third again indium was sputtered. The indium and tin film layer was 4 μm in thickness with indium 90% and tin 10% percentages. The highly doped p-type Si substrate was applied as gate to modulate the charge transfer. To fabricate ITO nanowires FET device, the as-grown thin film was patterned by E-beam lithography. Fig. 1 shows the pre-prepared nanowires FET schematically, (Fig. 1A and B). The thin film setup was sonicated in acetone and ultrasonically cleaned in ethanol and DI water. Main source and drain electrodes with spacing of 1 μm were defined by E-beam lithography. By preparing the source and drain electrodes, the growth of the nanowires was materialized. Then, the prepared thin film setup was heat treated in the tubular furnace (800°C) in gas presence (Ar:O_2 ratio 20:1) for 90 min. The schematic image of nanowires growth in the tubular furnace is shown in Fig. 1C and D.

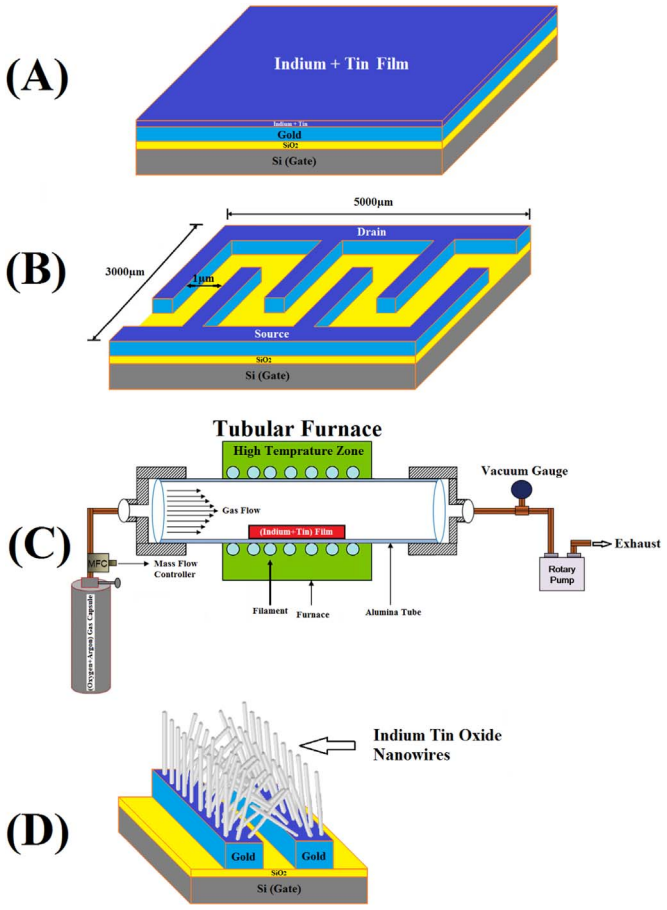

Fig. 1. The fabrication of ITO nanowires FET device. (A) The indium and tin film was coated on the gold film. The Si substrate with SiO_2 layer is the P-Type semiconductor and plays as a back-gate electrode. (B) The electrodes and FET pattern was defined by E-beam lithography. (C) The schematic image of tubular furnace. (D) The creation of nanowires in tubular furnace in under-controlled situation.

The oxidation process was performed under controlled vacuum circumstances. The applied technique used only In + Sn precursor materials with no challenges for nanofabrication process. The field emission scanning electron microscope (FESEM) (Hitachi model: S-4160) was used to characterize the morphology of nanowires and to demonstrate a prospective illustration of ITO nanowires FET. For crystallographic measurements, an X-ray diffracto-meter with CuKα line, 40 kV 100 mA, (model: Rigaku D/max RB) was used to characterize

crystalline structure of the products, see Fig. S4. For determining the morphology of the nanowires, and their sizes and directional growth intentions, a transmission electron microscopy (TEM) (model; Philips, CM-30) was used. For semiconductor measurements, HP4155B SPA the semiconductor parameter analyzer was used at room temperature.

2.3. The immobilization and hybridization of HBV DNA

The surface modification for HBV DNA probes immobilization on the Au-decorated nanowires was performed in a sterilized clean room. Immobilization of thiolated oligonucleotides probe initially was performed after DNA preparation by DTT. PBS (6 μL) (pH ~ 4.5) containing 100 μM single-stranded DNA probe was transported on the electrode, (modified nanowires) for 12 h. After DNA drop on the electrode surface, for removing some of the unabsorbed DNA oligonucleotides, the electrode system was submerged into 4 mM 6-mercapto-1-hexanol for 1hr and then cleansed by PBS and DDW.

For hybridization of SS-DNA probe with DNA target, first the probe electrode was submerged in PBS solution in pH ~ 7.5, in concentration of 15 μM SS-DNA target for 6hr. it is important to note; target was part of the DNA sequence of the HBV and it was a complementary strand to the DNA probe. Finally the sensing part of setup was cleansed with DDW and dried with argon gas in suitable flow. I_{DS}-V_{GS} was measured at constant bias voltage (V_{DS} = +3 V) while sweeping V_{GS} from ~ +5 V to + 17 V in steps of 0.1 V.

The stability and repeatability of the DNA biosensor was evaluated by storing the biosensor in a refrigerator at 4 °C for three and five weeks. After the hybridization and double strand formation, the biosystem was heated up to the satisfied value greater than the T_m (80 °C). For complete strands separation, they were quickly cooled down and washed up for target DNA removal from the ITO NWs surface. Then in final stage, the hybridization process and bio-sensing were repeated in the same condition method.

The response time, the detection range and detection limit were investigated. The probe concentration was kept constant at 10 μM and the DNA target was in 1 fM–10 μM concentration range, at room temperature. The ITO NWs response and output results were recorded at V_{DS} = +1 V; V_{GS} = +2 V. A clear change in drain current from 32 μA to 255 μA was observed when the injected target DNA was 1fM.

3. Results and discussion

3.1. Morphology, structure and phase

For characterizing the nanowires and discussing their morphology, phase and structure were measured by FESEM microscopy analysis. Fig. 2A demonstrates the typical field emission scanning electron microscopy images of the fabricated nanowires. Fig. 2A shows the fabricated indium tin oxide nanowires which were grown in tubular furnace. The shape of nanowires is exclusive, exactly grown on the gold thin film for FET application. These nanowires were able to connect to each other for transistor application as N-type semiconductor for channeling between source and drain. The size, detailed morphology and phase characterizations of the ITO nanowires were quantified by the TEM analysis. The transmission electron microscopy image of ITO nanowire shows that the nanowire is around 50 nm in diameter and several microns in length. The corresponding high resolution TEM image of the selected ITO nanowire is illustrated in Fig. 2B. In Fig. 2B, the HRTEM image indicates that the nanowire is highly crystalline and the crystallographic nature of the nanowire was calculated. The TEM shows that the tin dopant did not challenge the nanowire and there is no obvious dislocation or even cluster configuration. The high resolution TEM image confirms the cubic bixbyite structure of the indium tin oxide crystal. The two inter-plane distances were calculated and the lattice planes can be indexed to ITO (200). The lattice spacing of 0.507 nm for nanowire which is corresponding to (200) planes index,

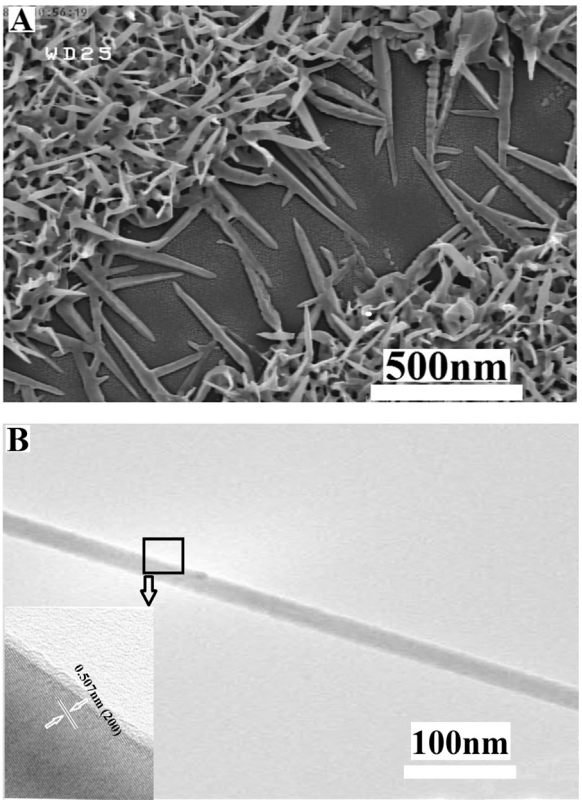

Fig. 2. (A) The FESEM images of ITO samples. The ITO nanowires were in the end of annealing process. Most of the nanowires were grown on the surface and some of them were able to form channel in FET configuration. (B) A bright field TEM image of ITO nanowires and the corresponding HRTEM image are shown. The HRTEM image is observed and can be indexed to ITO (200).

validates the In_2O_3 cubic phase.

3.2. The electrical responses of the FET biosensor to HBV DNA

The DNA immobilization and hybridization processes on the ITO nanowires were investigated. The detection of the DNA hybridization through ITO NWs FET electrical was confirmed. The biosensor responses of the HBV DNA were investigated via the carrier transfer properties of the ITO NWs FET after DNA immobilization is referenced to further investigations, (Fig. 3A). The hybridization bio-sensing quantifications were measured by amperometric technique. A 1fM concentration of the DNA oligonucleotides containing the complementary sequences was dropped on the ITO NWs FET surface. In the transfer curve study with probe and targets modifications (Fig. 3A), the curves show some current peaks/bands. This could be due to the coupling caused by induced electric field in the transistor, DNA type and the band gap of the channel material. After applying the potential driving force, the charged DNA sequences have been influenced by this electrical field and the coupling strengthens the flow response and makes sharp enhancement. Since the DNA oligonucleotides are in direct contact with the channel material, the oligonucleotides with larger values of electron negativity have greater adsorption strength with the channel material and stimulate the gating effect which is more likely to be dominant at a relatively low concentration.

The electrical transfer shift was observed because of the negatively-charged oligonucleotides complementary DNA targets. This shift is called the negative shift. The negative charge of DNA is due to the phosphate group of the DNA's backbone. The hybridization between probe and target caused transferring negative charges which highly influence the channel conductance in the FET system. These charges apply an electric field to the FET system. The applied electric field will

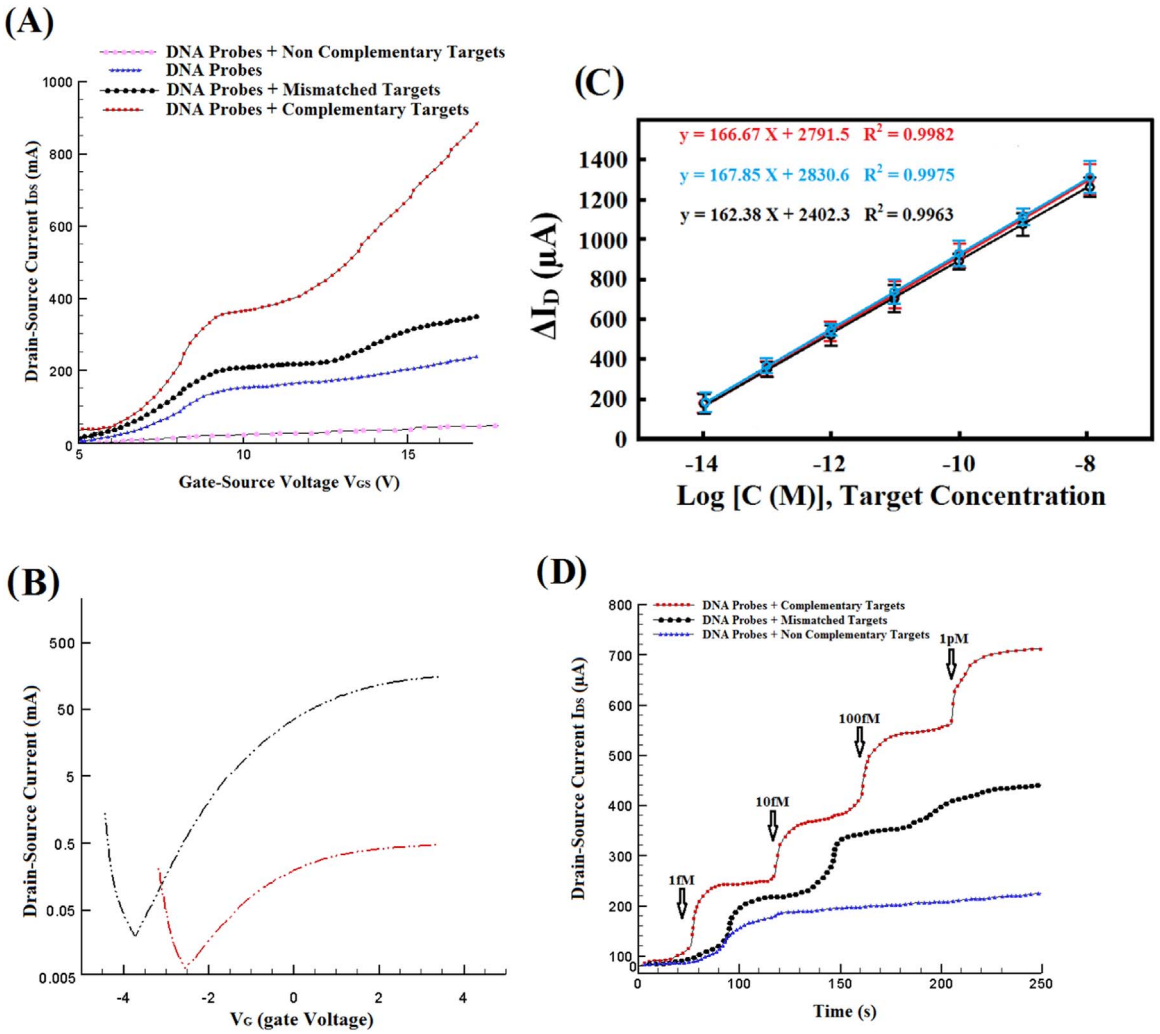

Fig. 3. (A) I_{DS}–V_{GS} curves obtained from a functionalized ITO NWs transistor after probes immobilization, after non-complementary, mismatch targets and then after hybridization of 1fM complementary targets. The constant V_{DS} was set at +3 V. (B) The transfer characteristics in which I_D was switched between "on" and "off" before (red curve) and after hybridization (black curve), V_{DS} = +3 V. (C) The relationship between current alterations and concentration, the lowest detection limit was 1fM. The stability and repeatability of the DNA biosensor for three (blue line) and five weeks (black line). The 98% and 96% of its initial response was achieved in the three and five weeks respectively. (D) The dynamic tests of FET biosensor. The dynamic tests of the sensor with complementary, non-complementary, and mismatch targets. The ITO NWs response and output results were recorded at V_{DS} = +1 V; V_{GS} = +2 V. (For interpretation of the references to color in this figure legend, the reader is referred to the web version of this article.).

stimulate the electrons flowing to the channel region, and causing the lower threshold voltage in the source-drain current vs. source-gate voltage plot for the ITO NWs FET performance. Also, the applied electric field will cause the current enhancement at fixed positive gate bias in the ITO NWs FET's channel. By increasing the concentration of the DNA oligonucleotides with accumulative negative charges, current in the channel increases. Consequently, we see in the I_{DS}–V_{GS} plot, a lower threshold voltage. For measuring the specificity of the biosensor, mismatched and non-complementary DNA oligonucleotides, hybridization of the targets with probes was checked. Weak interaction was achieved for non-complementary DNA oligonucleotides and electrical transfer characteristics did not change approximately. The relative good response for mismatched DNA oligonucleotides was recorded. This shows the ability of the biosensor to specify the complementary DNA targets from non-complementary and mismatched DNA oligonucleotides targets. Fig. 3B shows the transfer characteristics in which I_D was switched between "on" and "off" situation by altering potential of the gate (V_G) and the switching ratio between "on" and "off" state was $\sim 1.1 \times 10^5$. The results indicated that the specific DNA oligonucleotides were sensed by using the ITO NWs FET. In this way, the detection limit and the lowest detectable concentration have been measured. In Fig. 3C, the relationship between current alterations ($\Delta I_D = I_{D\ targets}$-$I_{D\ probes}$ for V_{GS} = 5 V) and concentration DNA is graphed. The logarithmic behavior of the biosensor was achieved. The lowest detection limit for detectable concentration quantity as small as 1fM was measured. This result shows the promised innovative ITO nanowires field effect transistor for DNA sensing with CMOS technology compatibility.

The stability and repeatability of the DNA biosensor were evaluated for three (blue line) and five weeks (black line), Fig. 3C. The results showed that the peak current of the biosensor retained 98% and 96% of its initial response for measurements after three and five weeks respectively.

The dynamic response of the biosensors to complementary DNA target is shown in Fig. 3D. In Fig. 3D, the ITO NWs FET-based DNA sensor responded to target concentrations of 1fM. It is completely obvious that the biosensor has demonstrated the high performance. The response time was 37 s.

To check the efficient probes immobilization, fluorescently DNA probes modified with fluorescein were immobilized and fluorescence images are observed. Initially, the biosensor was submerged in PBS and then in ethanol. Finally after heat treatment, the biosensor washed up by DIW. Fluorescently DNA probes modified with fluorescein are immobilized on unmodified surface and on functionalized surface.

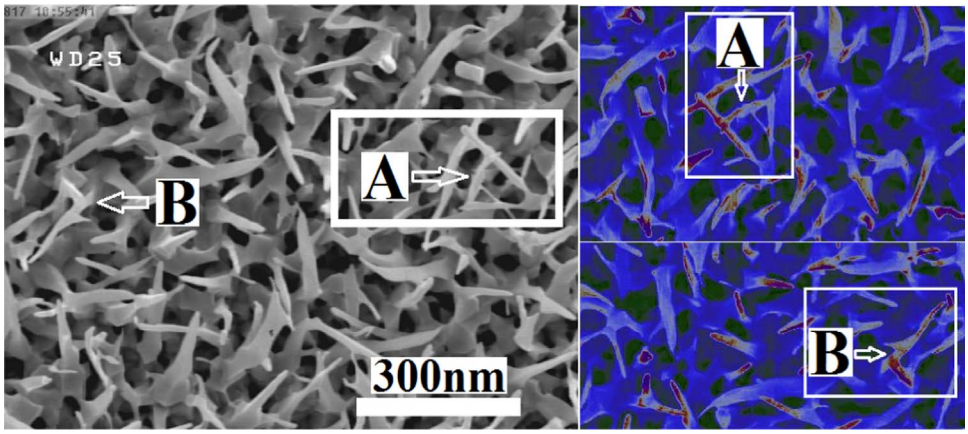

Fig. 4. The fluorescently DNA probes modified with fluorescein are immobilized and fluorescence images are observed, parts A and B are for correct validation and right navigation; the fluorescence image and related points are illustrated in the picture. The blue and violet backgrounds are due to preparation materials effects on the nanowires. (For interpretation of the references to color in this figure legend, the reader is referred to the web version of this article.).

Fluorescence images are observed to check the efficiency of probes immobilization. DNA strands cannot be linked on the nanowire without functionalization and thus the fluorescence was not observed on Fig. 4. The intensity of fluorescence on sample with functionalization suggests effective DNA strands immobilization (Fig. 4). Clear distinction of fluorescence is observed between unmodified and functionalized surface.

3.3. Discussion

The one-dimensional (1D) FET biosensors known as FET NWs biosensors have been demonstrated with intensive potential for the biological subjects sensing. Because of their ability to detect situ and tremendous electronic capabilities, nanowires have extremely been favored in bio-device configuration and detection, (Mao et al., 2017; Shariati, 2015, 2017). Although FET nanowires biosensors have been widely reported, very few practical applications or commercial products have been launched based on these FET sensors, (Mao et al., 2017). Major challenges limiting their practical applications include device-to-device variations and relatively high cost even in large-scale fabrication, (Mao et al., 2017; Ribovski et al., 2017). Compared with nanowires biosensors, two-dimensional ones (2D) can lead to conformal and intimate contact with metal electrodes, and they are easier to manipulate due to their relatively large lateral sizes, facilitating control over the channel structure in the FET detectors, (Mao et al., 2017). Also, 2D nano-sheets could be synthesized into designed shape and thickness and be precisely transferred onto the sensor configuration, (Mao et al., 2017).

The significant innovations which have been met in this research include the biosensor fabrication method, sensing mechanism and the control of the sensing conditions, including materials, rapid detection response and concentration. The fabricated biosensor has been scoped to measure the much lower concentrations. The fabricated biosensor also has the capability to connect the complementary metal–oxide–semiconductor (CMOS) technology to the integrated circuit system and to be commercially produced and deployed in detection systems. This biosensor measures the system current responses at relatively high rate, which makes it easier to optimize further future studies.

No substantial change in resistance was observed when a non-complementary or even a mismatched DNA target was exposed to the device that has a DNA probe covalently attached, which means that hardly any non-specific adsorption of DNA on the ITO NWs surface is detected, (Fig. 3A). In Table 1, the specific resistance change was investigated from hybridization of oligonucleotides to the ITO NWs device immobilized with DNA probe. As can be seen in Fig. 3A, a significant change (~ 58.2%) was observed when 1fM complementary target DNA was used, whereas only a negligible change was obtained when same concentration of non-complementary DNA was applied to

Table 1
The selectivity and specificity study. The summary of the sensor sensitivity to the DNA targets.

Hybridization	$(\frac{R-R_0}{R_0})\%$	RSD Value	Biosensor Stability (Dynamic Performance Time for 1 fM − 1 pM)
DNA Probe – DNA complementary target	58.2%	4.42%	10 min
DNA Probe – DNA mismatched target	25.1%	2.86%	3 min
DNA Probe – DNA non-complementary target	11.2%	0.37%	100 s

the ITO NWs device, (~ 14.2%). To evaluate the capability of the ITO NW device for discrimination of single base mismatches in DNAs, mismatched oligonucleotides were tested at 1 fM. The increase in resistance for mismatched DNA was ~ 23.1% which is much lower than that of complementary target DNA. The high specificity suggests that the ITO NWs device allows for label-free discrimination between the fully matched and mismatched DNAs, offering unique advantage over other technologies which require labeling and additional tags. The corresponding RSD values were 0.37% and 2.86% and 4.42% for non-complementary, mismatched and complementary target, respectively. The results indicate that the modified electrode has high reproducibility and excellent repeatability in both the preparation procedure and the sensing determinations. These results show the satisfying biosensor reaction to the specification and selectivity.

Table 2 shows the comparison of some field effect transistor NWs DNA biosensors (based on label as well as label-free detection). As seen in Table 2, the suggested sensor has a low detection limit and wide linear range, comparable to other DNA biosensors. It is believed that high surface area of ITO NWs and their specific structures with sharp edges associated with FET high performance are responsible for sensitive detection of HBV DNA.

4. Conclusion

The detailed fabrication procedure for the indium tin oxide nanowires field effect transistor biosensor is described. We demonstrate that this device can be used to detect the hepatitis B virus (HBV) in label free approach. This sensor has experimentally demonstrated its high sensitivity using synthetic sequences as probes and targets. The HBV DNA biosensor experimentally showed high sensitivity to detect the probes and targets. The biosensor was able to differentiate between complementary and non-complementary and mismatched sequences and the detection limits was 1fM. Thus the ITO NWs FET biosensor can be

Table 2
The Comparison of the different 1D nanostructures FET biosensors for DNA detection.

Biosensor	Capture probe (target length)	Limit of detection (LOD)	Linear Range	Technique Description	Reference
Quantitative real-time measurements of DNA hybridization with alkylated nonoxidized silicon nanowires in electrolyte solution	DNA (16 BP)	10 pM	10 pM – 100 nM	Electrostatically adsorbed capture probe, oxide layer removed by etching	Bunimovich et al., (2006)
Highly sensitive measurements of PNA-DNA hybridization using oxide-etched silicon nanowire biosensors	PNA (22 BP)	10 fM	10 fM – 1 μM	Oxide layer removed by chemical etching and SiNW surface passivated with an organic film	Zhang et al., (2008)
Label-free direct detection of MiRNAs with silicon nanowire biosensors.	PNA (22 BP)	1 fM	1 fM – 1 nM	Electrostatically neutral analog of DNA as a capture probe	Zhang et al., (2009)
Enhanced sensing of nucleic acids with silicon nanowire field effect transistor biosensors	DNA (24 BP)	0.1 fM	0.1 fM – 100 nM	Triangularly shaped SiNW-FETs operated at "subthreshold" regime	Gao et al., (2012)
Improving nanowire sensing capability by electrical field alignment of surface probing molecules.	DNA (15 BP)	0.1 fM	0. fM – 2 pM	Alignment of interfacial chemistry by electric field	Chu et al., (2013)
Silicon-Nanowire-Based CMOS-Compatible Field-Effect Transistor Nanosensors for Ultrasensitive Electrical Detection of Nucleic Acids	avian influenza DNA (25 BP)	1 fM of target DNA	(1 fM – 1 nM)	Small size of SiNWs achieved by implementation of NW structures with triangular cross section	Gao et al., (2011)
Carbon Nanotube Field-Effect Transistor for DNA Sensing	Influenza virus DNA (21 DNA BP)	1 pM	1 pM – 10 pM	using carbon nanotubes FET as the conducting channel (CNT-FET) has directly exposed to medium containing target DNA	Xuan et al., (2017)
Detection of influenza A virus using carbon nanotubes field effect transistor based DNA sensor	influenza A virus DNA (24 base pairs)	1 pM	1 pM – 10 nM	the probe single DNA strands immobilized to the CNT network and hybridize with the target DNA in an aqueous media leading to a change in the ion concentration at the interface	(Tran et al., 2017)
Precise and selective sensing of DNA-DNA hybridization by graphene/Si-nanowires diode-type biosensors	DNA	0.1 pM	0.1–500 nM	The CVD grown large-scale graphene/surface modified vertical-Si-NW-arrays junctions as diode-type biosensors for highly-sensitive and -selective detection of specific oligonucleotides.	Kim et al., (2016)

an interesting alternative to conventional DNA detectors detection because, in a few seconds, they can precisely analyze bio-molecular interactions in real time and in a label-free approach. The results were promising and trustable for developing the low cost, label-free and sensitive ITO NWs FET biosensor compatible with the CMOS technology. Next researches will focus on the disease detection by genetic mutation in bio-molecular studies, such as some cancer types related to inherited mutations.

Appendix A. Supporting information

Supplementary data associated with this article can be found in the online version at http://dx.doi.org/10.1016/j.bios.2018.01.022.

References

Bunimovich, Y.L., Shin, Y.S., Yeo, W.S., Amori, M., Kwong, G., Heath, J.R., 2006. Quantitative real-time measurements of DNA hybridization with alkylated non-oxidized silicon nanowires in electrolyte solution. J. Am. Chem. Soc. 128, 16323–16331.

Chu, C.J., Yeh, C.S., Liao, C.K., Tsai, L.C., Huang, C.M., Lin, H.Y., Shyue, J.J., Chen, Y.T., Chen, C.D., 2013. Improving nanowire sensing capability by electrical field alignment of surface probing molecules. Nano Lett. 13, 2564–2569.

Cui, Y., Wei, Q., Park, H., Lieber, C.M., 2001. Nanowire nanosensors for highly sensitive and selective detection of biological and chemical species. Science 293, 1289–1292.

Du, P., Li, H., Mei, Z., Liu, S., 2009. Electrochemical DNA biosensor for the detection of DNA hybridization with the amplification of Au nanoparticles and CdS nanoparticles. Bioelectrochemistry 75, 37–43.

Erdem, A., Kerman, K., Meric, B., Akarca, U.S., Ozsoz, M., 1999. DNA electrochemical biosensor for the detection of short DNA sequences related to the Hepatitis B virus. Electroanalysis 11, 586–587.

Fu, Y., Yuan, R., Xu, L., Chai, Y., Liu, Y., Tang, D., Zhang, Y., 2005. Electrochemical impedance behavior of DNA biosensor based on colloidal Ag and bilayer two-dimensional sol–gel as matrices. J. Biochem. Biophys. Methods 62, 163–174.

Furuberg, L., Mielnik, M., Gulliksen, A., Solli, L., Johansen, I., 2008. RNA amplification chip with parallel microchannels and droplet positioning using capillary valves. Microsyst. Technol. 14, 673–681.

Gao, A., Lu, N., Wang, Y., Dai, P., Li, T., Gao, X., Wang, Y., Fan, C., 2012. Enhanced sensing of nucleic acids with silicon nanowire field effect transistor biosensors. Nano Lett. 12, 5262–5268.

Gao, Anran, Lu, Na, Dai, Pengfei, Li, Tie, Pei, Hao, Gao, Xiuli, Gong, Yibin, Wang, Yuelin, Fan, Chunhai, 2011. Silicon-nanowire-based CMOS-compatible field-effect transistor nanosensors for ultrasensitive electrical detection of nucleic acids. Nano Lett. 11, 3974–3978.

Han, X., Fang, X., Shi, A., Wang, J., Zhang, Y., 2013. An electrochemical DNA biosensor based on gold nanorods decorated graphene oxide sheets for sensing platform. Anal. Biochem. 443, 117–123.

Jia, Z., Liu, J., Shen, Y., 2007. Fabrication of a template-synthesized gold nanorod-modified electrode for the detection of dopamine in the presence of ascorbic acid. Electrochem. Commun. 9, 2739–2743.

Kim, Jungki, Park, Shin-Young, Kim, Sung, Lee, Dae Hun, Kim, Ju. Hwan, Kim, Jong Min, Kang, Hee, Han, Joong-Soo, Park, Jun Woo, Lee, Hosun, Choi, Suk-Ho, 2016. Precise and selective sensing of DNA-DNA hybridization by graphene/Si-nanowires diode-type biosensors. Sci. Rep. 6, 31984.

Labuda, J., Brett, A.M.O., Evtugyn, G., Fojta, M., Mascini, M., Ozsoz, M., Palchetti, I., Palecek, E., Wang, J., 2010. Electrochemical nucleic acid based biosensors: concepts, terms, and methodology (IUPAC Technical Report). Pure Appl. Chem. 82, 1116–1187.

Mahoney, F.J., 1999. Update on diagnosis, management, and prevention of Hepatitis B Virus infection. Clin. Microbiol. Rev. 12, 351–366.

Mao, S., Chang, J., Pu, H., Lu, G., He, Q., Zhang, H., Chen, J., 2017. Two-dimensional nanomaterial-based field-effect transistors for chemical and biological sensing. Chem. Soc. Rev. 46, 6872–6904.

Nikoobakht, B., El-Sayed, M.A., 2003. Preparation and growth mechanism of gold Nanorods (NRs) using seed-mediated growth method. Chem. Mater. 15, 1957–1962.

Parab, H.J., Jung, C., Lee, J.H., Park, H.G., 2010. A gold nanorod-based optical DNA biosensor for the diagnosis of pathogens. Biosens. Bioelectron. 26, 667–673.

Patolsky, F., Zheng, G., Lieber, C., 2006. Nanowire-based biosensors. Anal. Chem. 78, 4261–4269.

Ribovski, L., Zucolotto, V., Janegitz, B.C., 2017. A label-free electrochemical DNA sensor to identify breast cancer susceptibility. Microchem. J. 133, 37–42.

Shakoori, Z., Salimian, S., Kharrazi, S., Adabi, M., Saber, R., 2015. Electrochemical DNA biosensor based on gold nanorods for detecting hepatitis B virus. Anal. Bioanal. Chem. 407 (2).

Shariati, M., Alishavandi, S., 2014. Phototransistor properties of indium tin oxide nanowires grown by rf sputtering mechanism and annealing process. Nano 10, 1550006.

Shariati, M., 2015. the continuous and persistent periodical growth induced by substrate accommodation in In_2O_3 nanostructure chains and their photoluminescence properties. Appl. Phys. A 118, 997–1007.

Shariati, M., 2017. The ITO-capped WO_3 nanowires biosensor based on field-effect transistor in label-free protein sensing. Appl. Phys. A 123, 370.

Shariati, M., Darjani, M., 2016. The lateral In_2O_3 nanowires and pyramid networks manipulation by controlled substrate surface energy in annealing evolution. J. Cryst. Growth 436, 104–112.
Sipova, H., Zhang, S., Dudley, A.M., Galas, D., Wang, K., Homola, J., 2010. Surface plasmon resonance biosensor for rapid label-free detection of microribonucleic acid at subfemtomole level. Anal. Chem. 82, 10110–10115.
Taylor, A.D., Ladd, J., Yu, Q.M., Chen, S.F., Homola, J., Jiang, S.Y., 2006. Quantitative and simultaneous detection of four foodborne bacterial pathogens with a multi-channel SPR sensor. Biosens. Bioelectron. 22, 752–758.
Tran, T.L., Nguyen, T.T., Tran, T.H., Chu, V.T., Tran, Q.T., Mai, A.T., 2017. Detection of influenza a virus using carbon nanotubes field effect transistor based DNA sensor. Physica E: Low-Dimens. Syst. Nanostructures 93, 83–86.
Wenga, G., Jacques, E., Salaun, A.-C., Rogel, R., Pichon, L., Geneste, F., 2013. Step-gate polysilicon nanowires field effect transistor compatible with CMOS technology for label-free DNA biosensor. Biosens. Bioelectron. 40, 141–146.
Wright, T.L., Lau, J.Y.N., 1993. Clinical aspects of hepatitis B virus infection. Lancet 342, 1340–1344.
Xuan, Chu T., Thuy, N.T., Luyen, T.T., Huyen, T.T., Tuan, M.A., 2017. Carbon nanotube field-effect transistor for DNAsensing. J. Electron. Mater. 46, 3507–3511.
Zhang, D., Peng, Y., Qi, H., Gao, Q., Zhang, C., 2010. Label-free electrochemical DNA biosensor array for simultaneous detection of the HIV-1 and HIV-2 oligonucleotides incorporating different hairpin-DNA probes and redox indicator. Biosens. Bioelectron. 25, 1088–1094.
Zhang, D., Chen, Y., Chen, H.Y., Xia, X.H., 2004. Silica-nanoparticle based interface for the enhanced immobilization and sequence specific detection of DNA. Anal. Bioanal. Chem. 379, 1025–1030.
Zhang, G.J., Chua, J.H., Chee, R.E., Agarwal, A., Wong, S.M., 2009. Label-free direct detection of MiRNAs with silicon nanowire biosensors. Biosens. Bioelectron. 24, 2504–2508.
Zhang, G.J., Chua, J.H., Chee, R.E., Agarwal, A., Wong, S.M., Buddharaju, K.D., Balasubramanian, N., 2008. Highly sensitive measurements of PNA-DNA hybridization using oxide-etched silicon nanowire biosensors. Biosens. Bioelectron. 23, 1701–1707.